



Resorbable Bone-Fixation Materials: Synthesis, Physical-Chemical and Biological Properties

Bakhtiniso Muzaffarova ¹, Sherzod Eranov ² and Sanjar Tillayev ^{*}

1. Department of Organic synthesis and Bioorganic chemistry, Samarkand State University named after Sharof Rashidov, Samarkand, Uzbekistan

2. Department of Traumatology and Orthopedics, Samarkand State Medical University, Samarkand, Uzbekistan

Abstract

Artificial bone materials were synthesized using the "solvent casting method" using polylactide/hydroxyapatite and various organic-inorganic modifiers. The physicochemical properties of the materials were studied using modern methods. IR spectroscopy showed that interactions between polymer macromolecules and hydroxyapatite occurred. When the powder was studied by the X-ray diffraction method, it was found to have an average crystallinity of 50-60%. When the textural properties were examined using SEM analysis, it was found that the introduction of magnesium phosphate into the samples resulted in the formation of porous particles with dimensions of 100-250 μm . This in turn, leads to the improvement of metabolic processes when the samples are introduced into living tissues. When the microhardness was determined by the Vickers method, it was found to be close to the hardness of natural bone, *i.e.* 27-34 HV. *In vitro* resorption was also performed in Simulated Body Fluids (SBF). Non-toxicity was observed when cytotoxic properties were studied. When the resorption process was studied *in vivo* in the upper third of the femur of rabbits, it was found that the ossification process of the samples was satisfactory after 28 days.

Keywords: Durapatite, Femur, Hydroxyapatite-polylactide, Lagomorpha, Porosity, Powders

To cite this article: Muzaffarova B, Eranov S, Tillayev S. Resorbable Bone-Fixation Materials: Synthesis, Physical-Chemical and Biological Properties. Avicenna J Med Biotech 2025;17(3): 196-207.

*** Corresponding author:**
Sanjar Tillayev, Ph.D.,
Department of Organic synthesis
and Bioorganic chemistry,
Samarkand State University
named after Sharof Rashidov,
Samarkand, Uzbekistan
Tel: +998 939983440
E-mail:
sanjar.tillayev83@gmail.com
Received: 15 Feb 2025
Accepted: 9 Jun 2025

Introduction

In recent years, the synthesis and application of biomedical materials with high compatibility with living cells, which make it possible to improve the outcomes of various injuries, as well whose properties are known prior to application, has become one of the urgent tasks. For example, the annual global demand for inert and resorbable plates and fixators used for the fixation of bone fractures is more than two million ¹. The most studied of such materials is based on collagen, a component of natural bone, and the mineral component calcium hydroxyapatite ^{2,3}. Another important component is polylactide, and its composite materials with the mineral component hydroxyapatite are also widely studied materials ^{4,5}. Also, researchers have developed resorbable composite materials designed to replace damaged bone tissue and their properties have been studied based on collagen/chitosan ⁶, nanocrystalline cellulose/polylactide ⁷, polyphosphazene/hydroxyapatite ⁸, poly- ϵ -caprolactone/calcium phosphate ⁹, agarose/hydroxyapatite ¹⁰ and a number of other materials.

A lot of research is being conducted on the production of resorbable biomedical materials. In particular, the production of materials that degrade over a certain period of time when filling bone injuries and dental defects in dentistry is one of the areas that has not lost its relevance. The most studied such materials are obtained on the basis of collagen, polylactide, chitosan, microcrystalline cellulose, ultra-high molecular weight polyethylene and other matrices ¹¹. One of the widely studied matrices is polylactide, and various methods have been used to improve the properties of materials based on it, such as the effect of polylactide stereoregularity ¹², the effect of nanosize and dispersity of hydroxyapatite particles ¹³, the effect of crosslinking polylactide macromolecules with D,L-lactide ¹⁴, modification of polylactide/hydroxyapatite composites with silver and carbon ¹⁵, the possibility of using polylactic acid and polyglycolide copolymers ¹⁶, modification of composite materials with nanodiamonds ¹⁷, the introduction of calcium carbonate into the poly(lactic acid) (PLA)/poly(butylene adipate-co-terephthalate) (PBAT)

matrix¹⁸, the use of polylactide and polymethyl methacrylate composites¹⁹, the effect of sucrose on the properties of polylactide/calcium carbonate composites²⁰, and a number of other methods. The properties of the resulting materials were studied in detail and their potential use for biomedical purposes was demonstrated.

It has been shown that it is possible to obtain artificial bone material by adding up to 1-4%²¹, 30%²², and up to 50%²³ of calcium hydroxyapatite to polylactide. The incorporation of up to 1% magnesium nanoparticles into the polylactide-graphite matrix has been shown to enhance the vitrification and crystallinity levels and porosity of the materials²⁴. These composite materials are suitable for fabricating customized biomedical implants using 3D printing technologies. It has been shown that the addition of fibrous magnesium metal to polylactide-based materials increases the mechanical strength of the material and ensures the release of limited amounts of Mg²⁺ ions²⁵. Spherical materials were obtained by adding collagen to polylactide/hydroxyapatite. The addition of collagen has been shown to improve the mechanical properties of materials¹¹. The addition of caprolactone to the polylactide/hydroxyapatite-based mixture has been shown to increase the mechanical strength of the resulting materials²⁶.

To obtain artificial bone materials, porous materials were obtained by biomimetic incorporation of apatite into a polylactide/calcium carbonate-based porous matrix in an alkaline environment²⁰. Porosity of approximately 75% and above gives the material osteoconductive properties (ensuring the conduction of bone tissue). However, it is important to note that the porosity of the material leads to a decrease in its mechanical properties. At the same time, it is important to obtain a material that is sufficiently porous and has a mechanical strength close to that of natural bone. Materials that are brittle compared to bone, because they cannot withstand heavy loads, prevent the achievement of the intended goals.

Polylactide-based resorbable materials have been employed in the treatment of segmental bone defects²⁷. Defects in various segments, such as the tibia (n=3), femur (n=4), and forearm (n=4), were studied in 11 patients with a mean age of 37 years (range 22-62 yr) treated by a single surgeon between 2010 and 2019. The average defect length was 6 cm, with a range of 3-12 cm. The etiology of the defects was osteomyelitis (n=7), oncological resection (n=3), and post-traumatic aseptic fusion (n=1). In experiments lasting an average of 24 months, polylactide-based membranes have shown positive results in the treatment of segmental bone defects up to 12 cm in size.

The possibility of using polylactide as a bone cement instead of traditional polymethyl methacrylate has been studied. The fact that 83% of osteogenic cells tested after solidification of granular PLA-based cement containing 80% of the material with a Molecular weight (Mw) of 10,770 retained viability, indicating that polylactide does not have cytotoxic properties and can be

used for these purposes²⁸. A resorbable, bioactive composite (POC-HA) based on poly (octamethylene citrate) (POC) and hydroxyapatite (HA) was obtained. While its mechanical properties were not inferior to existing analogues, when studied in human Mesenchymal Stem Cells (hMSC), it was noted that its osteogenic properties were significantly improved compared to currently widely used polylactide/hydroxyapatite-based materials²⁹.

Seven patients underwent surgery for long, radial bone fractures using resorbable "ActivaScrew™" screws made from polylactide-co-glycolide (PLGA)³⁰. No signs of excessive swelling, erythema, or adverse soft tissue responses were observed during the immediate postoperative period. The healing of broken bones of the patients for 3 months and more, the absence of additional complications was the basis for the conclusion that it is possible to recommend the use of these materials.

Although it has been shown that bone substitutes can be obtained by filling the polylactide matrix not only with hydroxyapatite, but also with other fillers, such as phosphate glass fiber (PBG/PLA)³¹, magnesium hydroxide³², and others, there is a need to expand the range of studies in this area and to conduct studies to evaluate the effect of various inorganic and organic modifiers on the physicochemical, mechanical, and biochemical properties of the materials.

The main research direction in recent years in this regard is the development of bone regeneration using modern "tissue engineering" methods^{33,34}. Despite advancements in tissue engineering, there remains a strong demand for cost-effective, easily manufacturable, resorbable biomaterials with high biocompatibility and compliance with clinical performance standards.

Despite certain achievements in the production of biomedical materials based on polylactide matrix and various fillers, there is a need to conduct comprehensive research on the production of materials with controlled degradation (or resorption) properties, improved physicochemical properties, sufficient mechanical strength, and high compatibility with blood and other biological fluids.

Based on the above, one of the important theoretical and practical tasks is to study the effect of various modifiers on the properties of resorbable composite materials based on polylactide/hydroxyapatite in biological environments.

Materials and Methods

Experimental

Materials: PLA (Mw=80 kDa), Calcium Hydroxyapatite (HA, particle size ~80 μm), MgF₂, CaF₂, Mg₃(PO₄)₂, citric acid, chloroform, and all reagents required for Simulated Body Fluids (SBF) were purchased from "Jinan Future Chemical Co." LTD, China.

Methods: Energy dispersion X-ray fluorescence analysis was used to determine the elemental composition of the samples (NexDe, Rigaku, Japan). To assess the

interaction of components in the synthesized composite material samples, IR spectra (IRAffinity-1S, Shimadzu, Japan) were studied. Parameters such as the degree of crystallinity and phase conditions of the samples were studied by the powder X-ray diffraction method. For this purpose, samples that were thoroughly ground into powder and passed through sieves were used. Powder X-ray diffractometer: Maxima, XRD-7000, Shimadzu, Japan. The analysis process is in CuK α electromagnetic radiation source, $\lambda=0.1544$ nm; 2nd scan from 10° to 70°; scanning step -0.02° ; speed -2°min^{-1} ; given voltage -30 kV, current -30 mA.

The morphological and textural characteristics of the synthesized biomedical composite materials were studied using a Scanning Electron Microscope (SEM). SEM images were obtained on an FEI microscope (NanoSEM 650 model, FEI Company) equipped with a TLC detector. The surfaces of the synthesized composite material samples were coated with a thin layer of gold by ion sputtering. The elemental composition of the samples in the studied area (surface) was also studied.

Complex thermal analysis of materials was carried out on a device (TG-60H, Shimadzu Corporation, Japan). The experiments were conducted at temperatures from 50 to 600°C, at a rate of $20^\circ \text{C min}^{-1}$, in a nitrogen atmosphere. The results were analyzed using the "Origin2024bSr0No_H" software.

DSC analysis of 8-16 mg samples of composite materials was carried out in a differential scanning calorimeter (DSC-60H, Shimadzu Corporation, Japan) in a nitrogen atmosphere, at a rate of $10^\circ \text{C min}^{-1}$. Based on the DSC analysis, the glass transition temperature (T_g), cold crystallization temperature (T_c) and crystallinity (X_c) of the samples were determined. The mechanical properties of the samples, in particular the hardness, were determined by the Vickers method (KASON-59-HVS, China).

When determining the hardness of samples using the Vickers method, a sample of the material being tested is subjected to a load (P) of up to 980.7 N (100 kgf) at an angle of 136° with a four-cornered pyramid-shaped diamond and held for 10-15 s. In these experiments, a load of 2 kg was applied to the samples and held for 20 s. Calculations were made according to the following formula:

$$H_D = 1,844 \frac{P}{D^2}$$

there: H_D – hardness, Vickers; P – applied load, kg; D – diagonal length of the end of the device intended for loading (average).

Determination of the cytotoxic properties of the synthesized samples was carried out according to the method presented in ³⁵. In this case, a test was performed on A549 and L929 cells using the 3-[4,5-dimethylthiazol-2-yl]-2,5-diphenyltetrazolium bromide (MTT) method.

The concentration of calcium ions in the SBF solutions was monitored using an atomic absorption spectrophotometer (AA-7000, Shimadzu, Japan). Tests in SBF: A modification of the method presented in ³⁶ was used to prepare the SBF solution. Egg albumin was used instead of human gamma globulins and human blood plasma albumin presented in this literature. The substances were dissolved in the amounts given in the table below in double-distilled water and the solutions were stored in a closed container, in the dark, at room temperature until the start of the experiments. The antimicrobial properties of the resulting composite materials were also determined by the disk diffusion method.

Synthesis of resorbable materials

The "solvent casting method" was used to obtain composite materials. For this, a certain amount of polylactide and calcium hydroxyapatite solutions in chloroform were used. The essence of the method is that a certain amount (10-12%) of polylactic acid was dissolved in the solvent with thorough mixing. Calcium hydroxyapatite sieved with a size of 0.075 μm and certain amounts of various modifiers were gradually added to it with constant stirring for 3-4 hr. The resulting mass was thoroughly mixed for 1-2 hr. The resulting contents are listed in table 1.

The resulting homogeneous mass was placed in open-mouthed containers to evaporate the solvent and left in the open air for 3-5 days. The resulting samples were processed by extrusion and brought to a cylindrical shape (Figure 1). Extrusion was carried out at $140 \pm 5^\circ \text{C}$.

Results and Discussion

Elemental analysis

The calcium hydroxyapatite samples used were of two types: one was a commercially obtained sample, and the other was a laboratory-synthesized sample. The

Table 1. Composition of synthesized composite materials

Composition	Amount added, mass %					
	PLA	HA	MgF ₂	CaF ₂	Mg ₃ (PO ₄) ₂	Citric acid
PLA/HA	80	20				
PLA/HA+MgF ₂	80	20	+20			
PLA/HA+CaF ₂	80	20		+20		
PLA/HA+Mg ₃ (PO ₄) ₂	80	20			+20	
PLA/HA+Citric acid	80	20				+20
PLA/HA+MgF ₂ +CaF ₂ +Mg ₃ (PO ₄) ₂	80	20	+6.67	+6.67	+6.67	
PLA/HA+MgF ₂ +CaF ₂ +Mg ₃ (PO ₄) ₂ +Citric acid	80	20	+5	+5	+5	+5

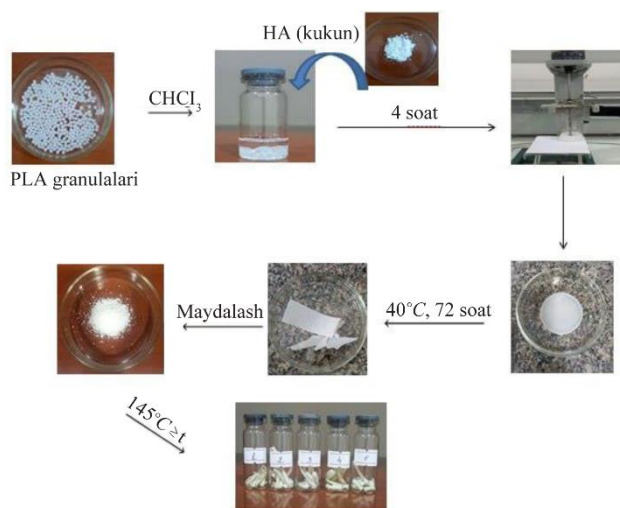


Figure 1. Scheme of obtaining biomedical composite materials based on PLA/HA and modifiers.

commercial HA sample was sieved using a $75\ \mu\text{m}$ mesh and used directly in the preparation of composite materials. The results of the elemental analysis of the synthesized samples showed that the molar ratios of CaO, MgO and P_2O_5 in their composition are as shown in table 2.

IR spectroscopy

The presence of a weak band in the region of $\sim 3250\text{--}3500\ \text{cm}^{-1}$ only in PLA/HA samples indicates a small number of functional groups related to O-H in the composition of the samples. Since the main O-H groups participate in the formation of complex ether bonds to form the polymer (Figure 2).

The alkane C-H stretching vibrations in the region below $3000\ \text{cm}^{-1}$, aliphatic complex ether bonds in the region of 1751.36 and $1718.58\ \text{cm}^{-1}$, strong bands at $\sim 1030\text{--}1040$ and $1082.07\ \text{cm}^{-1}$ are characteristic of the apatite lattice vibrations of the phosphate group. Usually, the stretching vibrations of the pure phosphate (PO_4^{3-}) group are visible in the region of $1024\ \text{cm}^{-1}$, and in these samples its appearance around the region of $\sim 1030\text{--}1040\ \text{cm}^{-1}$ indicates the occurrence of interactions between the polymer matrix and calcium hydroxyapatite. The changes caused by inorganic and organic substances introduced into the composition of the samples as modifiers are small. Only the appearance of a band in the region of $2358.94\ \text{cm}^{-1}$ in all samples with the addition of the modifier leads to the conclusion that

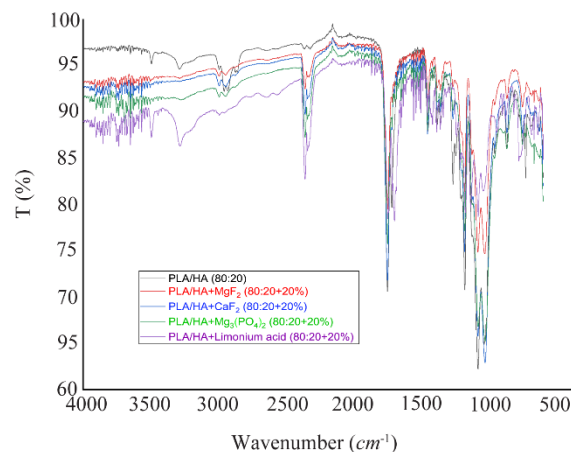


Figure 2. IR spectra of the samples.

it belongs to the asymmetric valence $\nu_1(\text{OH})$ vibrations of the free OH-groups in the samples. The shift of the bands characteristic of the C–O valence vibrations to 1182.36 , as well as the shift of the bands characteristic of the apatite lattice vibrations of the phosphate group to 1031.92 and $1083.99\ \text{cm}^{-1}$ allows us to conclude that interactions occurred between the polymer matrix and calcium hydroxyapatite. It can be noted that due to citric acid, bands characteristic of the free O–H groups appeared in the region of $3282.84\ \text{cm}^{-1}$ and in the regions of $\sim 3500\ \text{cm}^{-1}$ of the spectrum.

Powder X-ray diffraction

Figure 3 presents the comparative X-ray Diffraction (XRD) patterns of all synthesized samples. From the results obtained, we can see that the signals in the $2\theta = 15\text{--}20^\circ$ range belong to the α -phase of the high crystallinity region of PLA (pseudorhombic, $a = 1.06\ \text{nm}$)³⁷. The incorporation of various inorganic and organic modifiers into PLA/HA (80:20) composites alters the degree of crystallinity, as demonstrated in figure 3.

The observed peak broadening suggests a substantial amorphous phase within the composite matrix. The peaks in the $2\theta = 25\text{--}50^\circ$ range belong to calcium hydroxyapatite, and it can be seen that their intensities change depending on the nature of the added modifier. The X-ray diffraction pattern of the materials with 20% CaF_2 added as a modifier shows that the intensity of the peaks in the $2\theta = 15\text{--}20^\circ$ range decreased, and therefore the crystallinity decreased, but at the same time, new crystalline peaks were formed in the $2\theta = 30\text{--}60^\circ$ range. Although the addition of magnesium fluoride to the samples caused a decrease in the peaks corresponding to polylactide, it generally increased the crystallinity of the samples due to an increase in the number of crystal centers. It can be seen that the intensity of the peaks in the $2\theta = 15\text{--}20^\circ$ range increased relatively, but in the $2\theta = 30\text{--}60^\circ$ range, the peaks decreased and their intensity decreased compared to the samples with CaF_2 added. Citric acid incorporation led to reduced crystallinity, as

Table 2. Results of elemental analysis of the materials

Materials name	Content, mass %	CaO: MgO: P_2O_5
PLA/HA	80:20	4,3:0:1
PLA/HA+ MgF_2	80:20+20%	4,2:2,4:1
PLA/HA+ CaF_2	80:20+20%	6,6:0:1
PLA/HA+ $\text{Mg}_3(\text{PO}_4)_2$	80:20+20%	2,3:1,5:1
PLA/HA+Citric acid	80:20+20%	4,3:0:1

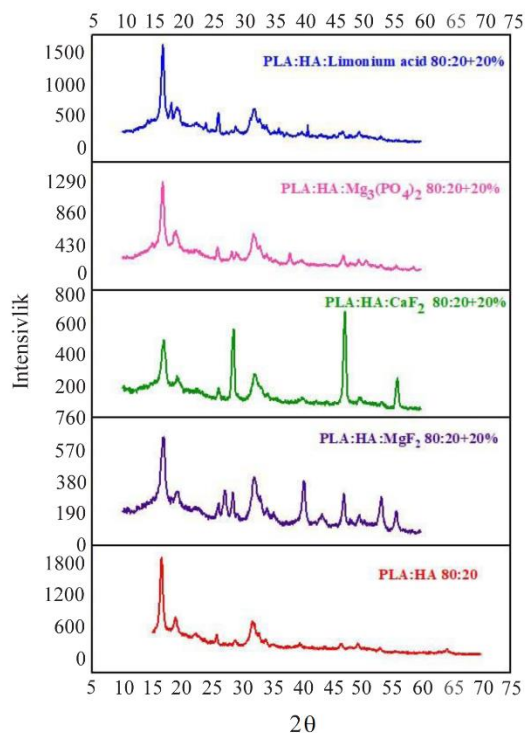


Figure 3. XRD results of the samples.

evidenced by diminished peak intensities and increased amorphous background in the diffraction pattern.

Based on the obtained diffractograms, the crystallinity of the samples was calculated. The crystallinity of the samples is presented in table 3. The results show that the crystallinity of the samples with magnesium fluoride as a modifier is high.

SEM analysis results

In the experiments, the surface morphology of materials with a PLA/HA ratio of 80/20 and samples with modifiers added in an amount of 10% by weight of the sample was studied (Figure 4). From the results obtained, we can see that PLA plays the role of the main matrix in the composition of the composite material. At this point, we can see from the elemental analysis results that the proportion of polylactide is higher than that of hydroxyapatite (1 mol of C atom corresponds to 1 mol of Ca atom). From the SEM analysis results obtained from another point of the composite material with a PLA/HA ratio of 80:20, the elemental analysis results at the point corresponding to the filler-calcium hydrox-

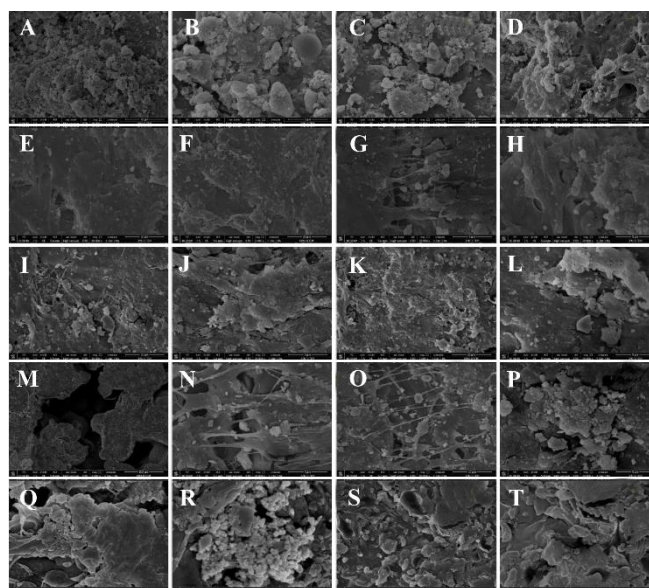


Figure 4. SEM analysis results of materials with PLA/HA 80:20 composition and 10% of various modifiers by mass of the sample.

yapatite also indicate that these granular associations are the result of agglomeration, association of calcium hydroxyapatite.

Figure 4 illustrates the influence of fillers on the microstructural and textural characteristics of the composite materials. From the analysis results, we can see that calcium hydroxyapatite nanocrystals aggregate and associate with each other, forming large structures (Figure 4A). These structures are 5-25 μm in size (Figures 4B and 4C), and the presence of micropores is clearly visible between them. It was observed that the size of the micropores lies in the region of 10-20 μm (Figures 4C and 4D). The abundance of micropores leads to a large relative surface area of the material. This, in turn, is considered to act as a conduit for cells and other nutrients during the process of bone tissue formation and accelerates the formation process³⁸.

From the SEM analysis results of materials obtained by adding 10% of MgF_2 by mass of samples with PLA/HA 80:20 composition, it can be seen that the adhesion of the components to each other is improved due to the addition of MgF_2 to the PLA/HA composites. From the elemental analysis results obtained at this point, it can be seen that the ratio of C:Ca atoms is approximately 10:1; and the ratio of C:Mg atoms is approximately 20:1. From the SEM analysis (Figures 4E-H) of composite materials with PLA/HA 80:20 composition and 10% MgF_2 by mass of the sample, it can be seen that the adhesion of calcium hydroxyapatite to the matrix is improved due to the added MgF_2 (Figures 4E and 4F). At the same time, the pores in the samples are also preserved (Figures 4G and 4H), the size of which is approximately 1-10 μm . As mentioned above, the pores act as a conduit for cells and other nutrients during the

Table 3. Effect of various modifiers on the crystallinity of the samples

Materials	Content, mass%	Crystallinity, %
PLA/HA	80:20	58.4
PLA/HA+ MgF_2	80:20+20%	60.6
PLA/HA+ CaF_2	80:20+20%	48.4
PLA/HA+ $\text{Mg}_3(\text{PO}_4)_2$	80:20+20%	53.2
PLA/HA+Citric acid	80:20+20%	53.7

process of bone tissue maturation and are considered to accelerate the maturation process.

SEM analysis of materials obtained by adding 10% CaF_2 to the samples with a PLA/HA ratio of 80:20 shows that the mutual adhesion of the components is improved due to the addition of CaF_2 to the PLA/HA composites, and the elemental analysis results show that the C:Ca atom ratio is approximately 6.8:1; the P:F atom ratio is approximately 8.3:1. From the analysis results, we can see that the porosity of the samples with the addition of CaF_2 is low (Figures 4I and 4J), and instead of it, microcrystalline granules with a size of 10-30 μm can be clearly seen. It was observed that the size of the existing pores is small, 5-10 μm . This allows us to conclude that the addition of calcium fluoride enhances the mutual aggregation of calcium hydroxyapatite and at the same time allows the granular microcrystals of calcium fluoride to separate separately.

SEM analysis of the materials obtained from the addition of 10% $\text{Mg}_3(\text{PO}_4)_2$ by mass of samples with a PLA/HA ratio of 80:20 shows that the introduction of magnesium phosphate into the sample composition leads to an increase in the size of the pores. At the examined point, it can be seen that the ratio of C:Ca atoms is 12.8:1, and the ratio of Ca:Mg is 1.8:1. The size of the pore spaces in the sample is large, reaching 100-250 μm (M), and the proportion of pores with a size of 5-20 μm is relatively small (Figures 4N and 4O). In addition, it can be seen that microcrystals of magnesium phosphate with a size of about 3-10 μm are separated in the sample (P). The addition of magnesium phosphate, on the one hand, enhances the adhesion and aggregation of calcium phosphate to the polylactide matrix, and on the other hand, increases the size of the pore spaces by ensuring the crystallization of aggregates at a certain size.

Based on the analysis results of samples obtained with the addition of 10% citric acid by mass to the samples, it can be seen that the C:Ca ratio increased slightly to 13.5:1 due to the addition of citric acid to the samples, *i.e.* due to the acid. We can see that the addition of citric acid to the samples improves the mutual adhesion of the components, but at the same time reduces the size of the pores in the material (Q). The size of the pores was around 2-10 μm (Figures 4Q and 4R). It can be observed that individual microcrystals of citric acid (and most

likely its calcium salt) with a size of 1-5 μm were formed in the composite.

From the above results, the following can be concluded: It was observed that the components added in an amount of 10% to the PLA/HA-based composite materials improved adhesion, with the best result being obtained with the addition of MgF_2 . Adhesion was slightly worse with the addition of citric acid compared to the control (Figure 5).

Since the porosity of materials affects the properties of the resulting biomedical product, when analyzing porosity, the best results were observed in samples with the addition of magnesium phosphate. The lowest porosity was found in samples with the addition of citric acid. From the above, it can be concluded that the addition of 10% magnesium phosphate or fluoride salts to PLA/HA-based samples has a positive effect on the adhesion and porosity of the samples.

Thermal analysis results

In order to evaluate the thermal properties of PLA (polylactide)/HA-based composite materials and the effect of the modifier included in the samples, complex thermal analysis studies were conducted. Samples with an optimally selected ratio of polylactide and calcium hydroxyapatite of 80:20 and samples with 5%, 10% and 20% MgF_2 , CaF_2 , $\text{Mg}_3(\text{PO}_4)_2$ and citric acid as modifiers were tested by thermal methods. The results were visualized and analyzed using the "Origin2024b Sr0No_H" software tool. The samples were ground and ground to a fine state using a special grinder, and the mass for analysis was obtained 9-13 mg.

Initially, samples of composite materials containing only PLA/HA in the mass ratio of 80:20–70:30–60:40 were analyzed. The main decomposition of the composite with a PLA/HA mass ratio of 80:20 began at 360°C. When the temperature reached 410°C, 77.23% of the sample decomposed and the residual ash content was 13.22%. Accordingly, endo-effects were observed at 290 and 410°C and exo-effects at 410, 470, 500 and 515°C. In the range of 100-200°C, a 3.95% mass loss was observed in the samples due to adsorbed water. From 200°C to 360°C, a 5.32% mass loss was observed due to volatile components in the sample-oligomers, solvent residues and other compounds. Therefore, thermal treatment of the samples at a temperature below the

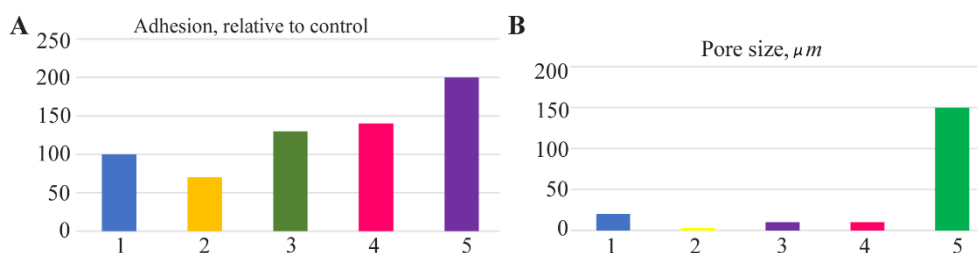


Figure 5. Adhesion (A) properties and porosity (B) of samples: A) 1-control; 2-citric acid; 3- $\text{Mg}_3(\text{PO}_4)_2$; 4- CaF_2 ; 5- MgF_2 . B) 1-control; 2-citric acid; 3- MgF_2 ; 4- CaF_2 ; 5- $\text{Mg}_3(\text{PO}_4)_2$.

glass transition temperature ($\sim 165^{\circ}\text{C}$) for a certain period of time can both increase their crystallinity and reduce the residual amount of solvent in them. When the PLA/HA mass ratios were 70:30 and 60:40, the ash content of the materials was 17.84 and 22.49%, respectively.

In the following experiments, the thermal properties of composite materials obtained by adding various modifiers that exhibit bioactivity to the samples were investigated. The effect of adding MgF_2 , CaF_2 , $\text{Mg}_3(\text{PO}_4)_2$ and citric acid as modifiers on the thermal properties of the materials was evaluated. For this, the effectiveness of adding the above modifiers to PLA/HA 80:20 samples in amounts of 5, 10 and 20% was evaluated.

In materials with MgF_2 as a modifier, the thermal stability exhibited minimal variation, but it can be seen that the amount of residual ash is directly related to the amount of modifier. It is also worth noting that the hygroscopicity has decreased.

It was observed that the addition of CaF_2 in an amount of 5, 10 and 20% by mass of the sample to PLA/HA 80:20 led to a decrease in the amount of main decomposition and an increase in the amount of residue. It had had minimal influence on endothermic and exothermic transitions. According to the results of thermal analysis of composite compounds with a composition of PLA/HA+ $\text{Mg}_3(\text{PO}_4)_2$ 80:20+5%, 10% and 20%, it can be concluded that the addition of $\text{Mg}_3(\text{PO}_4)_2$ as a modifier to the sample composition led to a decrease in the decomposition temperature of the main part of the compound (decreases to 260°C) and an increase in the amount of ash (up to 25%).

The addition of citric acid in the sample composition in the amount of 5, 10 and 20% by mass had almost no effect on the decomposition temperature, however, the lowest ash residue was achieved when 20% citric acid was added to the composition by mass. If we draw a general conclusion based on the results of thermal analysis of the above PLA/HA-based composite compounds, then the decomposition of the main part of the materials containing PLA/HA+ modifier was observed in the entire temperature range of $100\text{--}400^{\circ}\text{C}$ (Table 4). The temperature required for the decomposition of 70–80% of the compound is 360°C , which proves that the decomposition of polylactide, hydroxyapatite and fillers in the composition occurs at this temperature.

However, if we compare the data in the graphs and

tables above, we can see a sharp difference in the decomposition of $\text{Mg}_3(\text{PO}_4)_2$ and citric acid as fillers. The addition of $\text{Mg}_3(\text{PO}_4)_2$ to the composition of the mixture led to a sharp decrease in the decomposition temperature to 260°C . It can be seen that the addition of citric acid increased the amount of basic decomposition by 83.1%.

DSC analysis

From the results of DSC analysis, we can see that the glass transition temperatures of the obtained composite materials were within $165 \pm 3^{\circ}\text{C}$ (Figure 6). It can be seen that there was no significant change under the influence of the added modifiers.

Microhardness test of materials by vickers

Two types of samples were used to determine the microhardness of the samples. First, the hardness of the materials obtained by evaporation from solutions was studied (Figure 7). It was observed that the microhardness of the obtained materials was between 13.0 and 15.7 HV. This value is significantly lower than the hardness range of 28–50 HV, which varies depending on

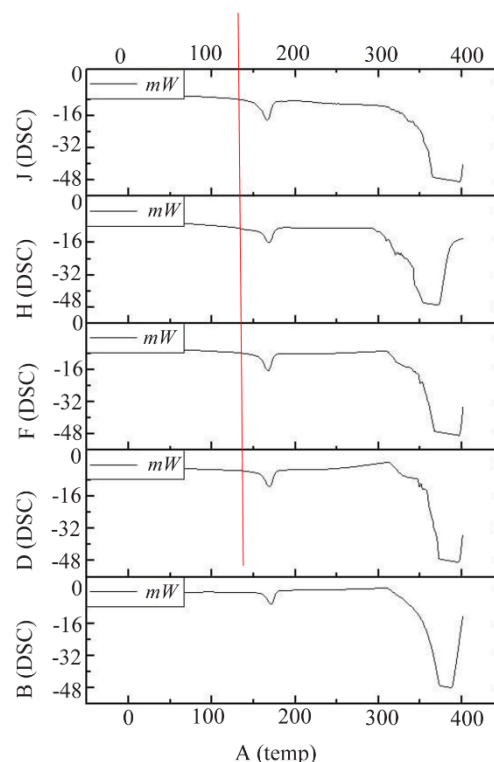


Figure 6. Glass transition points of samples.

Table 4. Comparative thermal properties of the samples

Materials composition	Content, mass %	Main mass lose temperature, $^{\circ}\text{C}$	Main decomposition rate (%)	Ash content (%)
PLA/HA	80:20	360	77.23	13.22
PLA/HA/ MgF_2	80:20:20	365	73.09	15.06
PLA/HA/ CaF_2	80:20:20	365	70.72	16.4
PLA/HA/ $\text{Mg}_3(\text{PO}_4)_2$	80:20:20	260	66.24	25.02
PLA/HA/citric acid	80:20:20	365	83.1	5.83

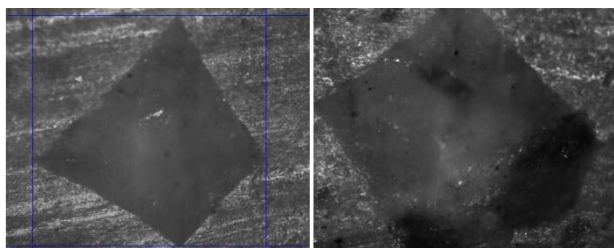


Figure 7. Determination of microhardness of samples by Vickers.

the age of the person and the type of bone. Therefore, the samples were extruded to increase the degree of crystallinity, and therefore the hardness, as well as to carry out the shaping process. As a result of extrusion, it can be seen that the microhardness of the samples increased to 27-34 HV (Table 5). The hardest samples were found to be those with 5% each of MgF_2 + CaF_2 + $\text{Mg}_3(\text{PO}_4)_2$ added to the PLA/HA-based composite.

The addition of a modifier to the samples increases the hardness compared to pure PLA/HA. It was observed that the hardness increased depending on the amount of added modifier in the order $\text{MgF}_2 < \text{CaF}_2 < \text{Mg}_3(\text{PO}_4)_2$. It was found that when equal amounts of modifiers were added, the compositions with the addition of $\text{Mg}_3(\text{PO}_4)_2$ had the hardest structure, allowing to obtain samples equal to or harder than the minimum hardness of natural bone –28 HV.

Tests in SBF

A modification of the Kokubo method was used to prepare the body fluid simulation solution. Instead of human gamma-globulins and human blood plasma albumin presented in this literature, egg albumin was used (Table 6).

The substances were dissolved in double-distilled water in the amounts given in the table 6 and the solutions were stored in a closed container, in the dark, at room temperature until the start of the experiments. In the experiments, the synthesized material samples were placed in a bag consisting of a semiconductor membrane, immersed in the prepared SBF and left in a thermostat at a constant temperature of 37°C, with occasional shaking.

First, a certain aliquot of the liquid in the flasks was taken every 3 hr during the first 3 days, every 6 hr on days 4-7, every 12 hr on days 8-20, and once every 5

Table 6. Composition of SBF solution

No	Ion	Ion concentration, (mM)
1	Na^+	142.0
2	HCO_3^-	4.2
3	K^+	5.0
4	HPO_4^{2-}	1.0
5	Mg^{2+}	1.5
6	Cl^-	148.8
7	Ca^{2+}	2.5
8	SO_4^{2-}	0.5

days, and the samples were analyzed for calcium ion. The concentration of calcium ion in the solutions was monitored with an atomic absorption spectrophotometer. According to the analysis results, the degradation properties of the synthesized samples were evaluated (Figure 8).

According to the results of 150-day experiments, it was found that the fastest degradation was in samples where citric acid was used as a modifier, and the slowest degradation was in samples with the addition of magnesium phosphate. The time taken for half ($\Delta m/2$) of the material samples to degrade was 70-127 days. The fastest half-life was observed in samples with added citric acid (70 ± 2 days), and the slowest degradation was observed in samples with added magnesium phosphate (127 ± 3 days).

Study of cytotoxic properties

For this, cells were seeded in a 96-well plate with 104 cells per well ³⁵. After 24 hr, the medium was removed from the tablet well. After that, the studies were continued with media containing the synthesized materials at the following concentrations: 62.5 µg/ml; 125 µg/ml; 250 µg/ml; 500 µg/ml; 1000 µg/ml. Standard media were added to control wells and incubated for 24 hr. After incubation, 20 µl of MTT (5 mg/ml in phosphate buffer) was added to the wells. After 4 hr, this solution was removed from the wells and replaced with 200 µl of DMSO. The optical activity of each well was measured at a wavelength of 540 nm. According to the optical densities of the samples, the viability of the cells in each well was calculated in % compared to the control sample. The obtained results are presented in figure 9. From the obtained results, it can be seen that the synthesized samples showed almost no cytotoxic pro-

Table 5. Hardness of samples after synthesis and after extrusion

Materials	Content, %	Microhardness, by Vickers, HV	
		After synthesis	After extrusion
PLA/HA	80:20	13,2±0.1	28,1±0.2
PLA/HA+ MgF_2	80:20+20%	13,5±0.1	29,7±0.2
PLA/HA+ CaF_2	80:20+20%	14,2±0.2	31,5±0.3
PLA/HA+ $\text{Mg}_3(\text{PO}_4)_2$	80:20+20%	15,5±0.1	32,6±0.2
PLA/HA+ citric acid	80:20+20%	13,0±0.2	27,3±0.1
PLA/HA + MgF_2 + CaF_2 + $\text{Mg}_3(\text{PO}_4)_2$	80:20+5+5+5	15,7±0.1	34,4±0.2

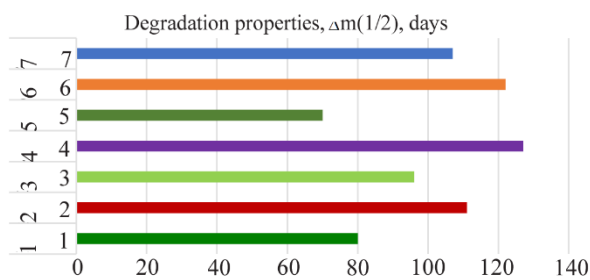


Figure 8. Degradation characteristics of synthesized materials in SBF.

properties compared to the control samples. In particular, it was found to have no significant effect on A549 cells. In tests conducted on L929 cells, it was observed that at high concentrations, 52-60% of viability was maintained compared to the control medium.

Determination of antimicrobial activity

For this, 3 different strains of micro-organisms were used: *Staphylococcus aureus* (*S. aureus*), *Escherichia coli* (*E. coli*), and *Candida albicans* (*C. albicans*)^{39,40}. Viable strains of micro-organisms were inoculated into sterilized Petri dishes (diameter 12 mm). The plate contains Mueller-Hilton (Merck) agar medium and its concentration corresponds to a 0.5 McFarland turbidity standard level (106-107 CFU/ml). Dispersions, each containing 10 µg of test sample, were poured onto a sterile blank disc in a Petri dish. A disc containing penicillin (5 IU) was selected as a control. After the samples were added, the discs were incubated at 37°C for 24 hr. Inhibited zones around the discs were measured using a digital caliper and expressed in mm. From the obtained results, it was observed that the samples have antimicrobial properties compared to penicillin.

Study of the resorption properties of samples in vivo

In order to study the condition of the samples when they were inserted into the bone, the upper third of the femur of experimental rabbits was determined. The operation was carried out in the operating room of the Veterinary and Animal Husbandry Development Department of Samarkand city. The right and left legs of the experimental rabbits were selected for the main and

control groups, where the right leg of the experimental rabbit was designated as the main group and the left leg as the control group. Operation process: Under general anesthesia, the area of the upper third of both legs was cleaned of hair. The skin of the upper third of the right thigh was excised in layers, measuring 1.5 cm (Figure 10).

The periosteum was separated, a hole was made in the bone using a 2 mm drill, and the specimen was inserted into the hole. The soft tissues were sutured in layers, the skin was incised, and the wound was closed with an aseptic bandage (Figure 11).

The skin of the upper third of the left thigh was incised 1.5 cm in layers, the periosteum was separated, a hole was made in the bone using a 2 mm drill, and the soft tissues were sutured in layers, the skin was sutured, and aseptically bandaged. The left thigh served as a control, as described above. According to the results of the examination 28 days after the operation, the operative wound is completely healed (Figure 12). The control radiograph shows satisfactory pattern and ossification process in the upper third of the right femur, but slow ossification process in the hole formed in the upper third of the left femur.



Figure 10. The process of making a hole in the bone using a 2 mm drill.



Figure 11. The process of inserting a sample into a hole made in the bone and suturing the skin.

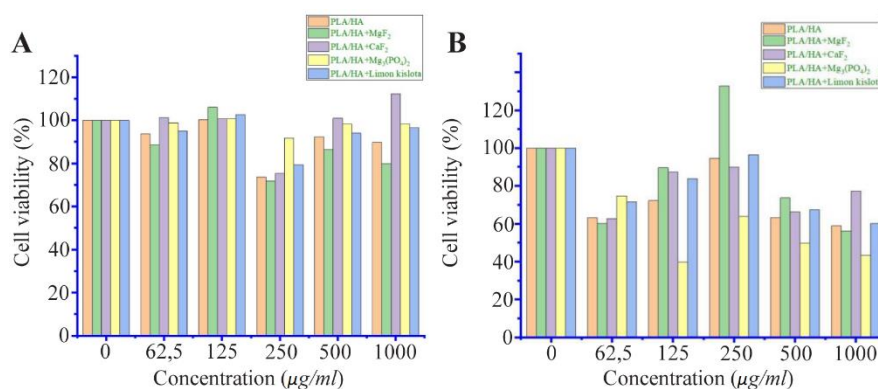


Figure 9. Results of cytotoxicity assays against A549 (A) and L929 (B) cells.



Figure 12. The result after 28 days, clinical appearance and X-ray.

Conclusion

Biomedical composite materials with resorbable properties, bone substitutes, were synthesized using the "solvent casting method" based on polylactide and calcium hydroxyapatite, as well as various inorganic modifiers. The physicochemical properties of the materials were studied using modern methods: ERF, XRD, FTIR, TGA, DSC, and the mechanical hardness was studied using the Vickers method. IR spectroscopy showed that interactions between polymer macromolecules and hydroxyapatite occurred. When the powder was studied by the X-ray diffraction method, it was found to have an average crystallinity of 50-60%. When the textural properties were examined using SEM analysis, it was found that the introduction of magnesium phosphate into the samples resulted in the formation of porous particles with dimensions of 100-250 μm . This in turn, leads to the improvement of metabolic processes when the samples are introduced into living tissues. When the microhardness was determined by the Vickers method, it was found to be close to the hardness of natural bone, *i.e.* 27-34 HV. *In vitro* resorption was also performed in SBF. Depending on the nature of the modifier in the sample, it was observed that the time taken for 50% degradation of the samples ranged from 60 to 150 days. Non-toxicity was observed when cytotoxic properties were studied. When the resorption process was studied *in vivo* in the upper third of the femur of rabbits, it was found that the ossification process of the samples was satisfactory after 28 days.

Ethical Approval

All applicable international and/or national guidelines for the care and use of animals, as well as the guidelines of the institution in which the study was performed, were followed. All procedures performed in studies involving animals were in accordance with the ethical principles 15 and 16 of the codes of ⁴¹ generally accepted practice for such research and were reviewed with the ethical committee of Samarkand State Medical University.

Acknowledgement

The authors express their gratitude for valuable advice and appropriate infrastructure for conducting

medical operations related to the implantation of the synthesized biomaterials to the Ethical Council of the Samarkand State Medical University and the Samarkand City Department of Veterinary Medicine and Animal Husbandry of the Ministry of Agriculture of the Republic of Uzbekistan. No conflicts of interest were declared by the authors.

Conflict of Interest

All authors made equal contributions to the writing of the article.

References

1. Campana V, Milano G, Pagano E, Barba M, Cicione C, Salonna G, et al. Bone substitutes in orthopaedic surgery: from basic science to clinical practice. *J Mater Sci Mater Med* 2014 Oct;25(10):2445-61.
2. Chai Y, Okuda M, Otsuka Y, Ohnuma K, Tagaya M. Comparison of two fabrication processes for biomimetic collagen/hydroxyapatite hybrids. *Advanced Powder Technology* 2019 Jul 1;30(7):1419-23.
3. Irawan V, Kajiwaru D, Nakagawa Y, Ikoma T. Fabrication of mechanically robust bilayer membranes of hydroxyapatite/collagen composites. *Materials Letters* 2021 May 15;291:129514.
4. Çelik T, Saraçoğlu B, Özkan A, İlhan Y. Biodegradable PLA/Ha Composite Material Production and Mechanical Characterization for Temporary Implant Applications. *International Journal of Pioneering Technology and Engineering* 2023 Dec 15;2(02):188-92.
5. Aihemaiti P, Jiang H, Aiyiti W, Wang J, Dong L, Shuai C. Mechanical properties enhancement of 3D-printed HA-PLA composites using ultrasonic vibration assistance. *Virtual and Physical Prototyping* 2024 Dec 31;19(1):e2346271.
6. Li M, Jia W, Zhang X, Weng H, Gu G, Chen Z. Hyaluronic acid oligosaccharides modified mineralized collagen and chitosan with enhanced osteoinductive properties for bone tissue engineering. *Carbohydr Polym* 2021 May 15;260:117780.
7. Luo W, Cheng L, Yuan C, Wu Z, Yuan G, Hou M, et al. Preparation, characterization and evaluation of cellulose nanocrystal/poly(lactic acid) in situ nanocomposite scaffolds for tissue engineering. *Int J Biol Macromol* 2019 Aug 1;134:469-479.
8. Nukavarapu SP, Kumbar SG, Brown JL, Krogman NR, Weikel AL, Hindenlang MD, et al. Polyphosphazene/nano-hydroxyapatite composite microsphere scaffolds for bone tissue engineering. *Biomacromolecules* 2008 Jul;9(7):1818-25.
9. ShiraliPour F, Shafiei SS, Nikakhtar Y. Three-dimensional porous poly(ϵ -caprolactone)/beta-tricalcium phosphate microsphere-aggregated scaffold for bone tissue engineering. *International Journal of Applied Ceramic Technology* 2021 Sep;18(5):1442-56.
10. Khosalim IP, Zhang YY, Yiu CKY, Wong HM. Synthesis of a graphene oxide/agarose/hydroxyapatite biomaterial with the evaluation of antibacterial activity and initial cell attachment. *Sci Rep* 2022 Feb 4;12(1): 1971.

11. Zhang Y, Wang W, Chen Z, Shi H, Zhang W, Zhang X, et al. An artificial bone filling material of poly l-lactic acid/collagen/nano-hydroxyapatite microspheres: Preparation and collagen regulation on the property. *Int J Biol Macromol* 2023 Feb 28;229:35-50.
12. Soloveva Vera Aleksandrovna. Composites on the basis of biodecomposed polymers for implantatov in maxillofacial surgery: Dissertation. Chem.Sci. 05.17.06 Moscow, 2005 150 p.
13. Boruvka M, Cermak C, Behalek L, Brdlik P. Effect of in-mold annealing on the properties of asymmetric poly (L-lactide)/poly (D-lactide) blends incorporated with nano-hydroxyapatite. *Polymers* 2021 Aug 23;13(16):2835.
14. Targonska S, Dobrzynska-Mizera M, Wujczyk M, Rewak-Soroczynska J, Knitter M, Dopierala K, et al. New way to obtain the poly (L-lactide-co-D, L-lactide) blend filled with nanohydroxyapatite as biomaterial for 3D-printed bone-reconstruction implants. *European Polymer Journal* 2022 Feb 15;165:110997.
15. Vasenina IV, Savkin KP, Laput OA, Lytkina DN, Botvin VV, Medovnik AV, et al. Effects of ion-and electron-beam treatment on surface physicochemical properties of polytetrafluoroethylene. *Surface and Coatings Technology* 2018 Jan 25;334:134-41.
16. Parker NG, Mather ML, Morgan SP, Povey MJ. Longitudinal acoustic properties of poly(lactic acid) and poly (lactic-co-glycolic acid). *Biomed Mater* 2010 Oct;5(5): 055004.
17. Cai N, Dai Q, Wang Z, Luo X, Xue Y, Yu F. Preparation and properties of nanodiamond/poly (lactic acid) composite nanofiber scaffolds. *Fibers and Polymers* 2014 Dec; 15:2544-52.
18. Teamsinsungvon A, Ruksakulpiwat Y, Jarukumjorn K. Poly (lactic acid)/Poly (butylene adipate-co-terephthalate) Blend and its Composite: Effect of Maleic Anhydride Grafted Poly (lactic acid) as a Compatibilizer. *Advanced Materials Research* 2012 Feb 15;410:51-4.
19. Vu MC, Jeong TH, Kim JB, Choi WK, Kim DH, Kim SR. 3D printing of copper particles and poly (methyl methacrylate) beads containing poly (lactic acid) composites for enhancing thermomechanical properties. *Journal of Applied Polymer Science* 2021 Feb 5;138(5):49776.
20. Maeda H, Kasuga T, Nogami M. Bonelike apatite coating on skeleton of poly (lactic acid) composite sponge. *Materials Transactions* 2004;45(4):989-93.
21. Pandele AM, Constantinescu A, Radu IC, Miculescu F, Ioan Voicu S, et al. Synthesis and Characterization of PLA-Micro-structured Hydroxyapatite Composite Films. *Materials (Basel)* 2020 Jan 8;13(2):274.
22. Albano C, González G, Palacios J, Karam A, Castillo RV, Covis M. Characterization of poly l-lactide/hydroxyapatite composite: Chemical, thermal and thermomechanical properties. *Revista de la Facultad de Ingeniería Universidad Central de Venezuela* 2013 Sep;28(3):97-107.
23. Zare RN, Doustkhah E, Assadi MH. Three-dimensional bone printing using hydroxyapatite-PLA composite. *Materials Today: Proceedings* 2021 Jan 1;42:1531-3.
24. Mohammadi-Zerankeshi M, Alizadeh R. 3D-printed PLA-Gr-Mg composite scaffolds for bone tissue engineering applications. *Journal of Materials Research and Technology* 2023;22:2440-6.
25. Sun S, Gao L, Liang B, Yin Z, Pan S, Shi C, et al. Long-term and uniform release of magnesium ions from PLA porous composite materials oriently reinforced by Mg wires for potential bone repair application. *Surfaces and Interfaces* 2023 Aug 1;40:103018.
26. Jodeh S, Azzaoui K, Mejdoubi E, Lamhamdi A, Hammouti B, Akartasse N, et al. Novel tricomponenets composites films from polylactic acid/hydroxyapatite/poly-caprolactone suitable for biomedical applications. *J. Mater. Environ. Sci.* 2016;7: 761-9.
27. Nahm NJ, Conway JD. Resorbable polylactide membrane for the treatment of segmental bone defects. *Injury* 2022 Feb;53(2):376-80.
28. Channasanon S, Kaewkong P, Tanodekaew S. Dual-Curing Polylactide for Resorbable Bone Cement. *Key Engineering Materials* 2019 May 10;798:77-82.
29. Thirumaran A, Doulgkeroglou MN, Sankar M, Easley JT, Gadowski B, Poudel A, et al. A functional analysis of a resorbable citrate-based composite tendon anchor. *Bioact Mater* 2024 Jul 22;41:207-20.
30. Pierre Lascombes, Pierre Journeau, Dmitry A. Popkov. Resorbable implants in paediatric orthopaedics and traumatology. *Genij Ortopedii* 2023;29(6):629-34.
31. Harper LT, Ahmed I, Felfel RM, Qian C. Finite element modelling of the flexural performance of resorbable phosphate glass fibre reinforced PLA composite bone plates. *J Mech Behav Biomed Mater* 2012 Nov;15:13-23.
32. Guo W, Bu W, Mao Y, Wang E, Yang Y, Liu C, et al. Magnesium Hydroxide as a Versatile Nanofiller for 3D-Printed PLA Bone Scaffolds. *Polymers (Basel)* 2024 Jan 9;16(2):198.
33. Serim TM, Amasya G, Eren-Böncü T, Şengel-Türk CT, Özdemir AN. Electrospun nanofibers: building blocks for the repair of bone tissue. *Beilstein J Nanotechnol* 2024 Jul 25;15:941-53.
34. Hwang HS, Lee CS. Nanoclay-Composite Hydrogels for Bone Tissue Engineering. *Gels* 2024 Aug 3;10(8):513.
35. Erol I, Mutlu T, Hazman Ö, Khamidov G. Effect of a new methacrylate polymer with chlorobenzyl amide side group and biosynthesized ZnO nanoparticles on thermal and biological properties of chitosan. *Cellulose* 2024 Sep;31 (14):8587-608.
36. Gligorijević BR, Vilotijević MN. Simulated body fluids prepared with natural buffers and system for active pH regulation. *Iranian Journal of Chemistry and Chemical Engineering* 2022;41(9):2918-35.
37. Luo W, Cheng L, Yuan C, Wu Z, Yuan G, Hou M, et al. Preparation, characterization and evaluation of cellulose nanocrystal/poly(lactic acid) in situ nanocomposite scaffolds for tissue engineering. *Int J Biol Macromol* 2019 Aug 1;134:469-79.
38. Wee CY, Yang Z, Thian ES. Past, present and future

- development of microspheres for bone tissue regeneration: a review. *Materials Technology* 2021 May 12;36 (6):364-74.
39. Sivrier M, Hazman Ö, Tillayev S, Erol I. Novel bionanocomposites containing green synthesized silver NPs of a carboxymethyl cellulose-based blend; thermal, optical, biological and dielectric properties. *Journal of Polymers and the Environment* 2023 Sep;31(9):3857-74.
40. Hazman Ö, Khamidov G, Yilmaz MA, Bozkurt MF, Kargioğlu M, Tukhtaev D, et al. Environmentally friendly silver nanoparticles synthesized from *Verbascum nudatum* var. extract and evaluation of its versatile biological properties and dye degradation activity. *Environ Sci Pollut Res Int* 2024 May;31(23): 33482-94.
41. Guidelines for research ethics in science and technology// National Committee for Research Ethics in Science and Technology, Norway, Oslo, 3rd Edition, 2024.